

MASTER**Optical Properties of Metals by Spectroscopic Ellipsometry*****E. T. Arakawa, T. Inagaki,⁺ and M. W. Williams****Health and Safety Research Division
Oak Ridge National Laboratory
Oak Ridge, Tennessee 37830**

By acceptance of this article, the publisher or recipient acknowledges the U.S. Government's right to retain a nonexclusive, royalty-free license in and to any copyright covering the article.

NOTICE

This report was prepared as an account of work sponsored by the United States Government. Neither the United States nor the United States Department of Energy, nor any of its employees, makes any warranty, express or implied, or assumes any legal liability for the accuracy, completeness, or usefulness of any information, product, or process disclosed, or represents that its use would not infringe upon privately owned rights.

***Research sponsored by the Office of Health and Environmental Research, U. S. Department of Energy, under contract W-7405-eng-26 with the Union Carbide Corporation.**

⁺Present address: Department of Physics, Osaka Kyoiku University, Tennoji, Osaka, Japan.

Optical Properties of Metals by Spectroscopic Ellipsometry

E. T. Arakawa, T. Inagaki,* and M. W. Williams
Health and Safety Research Division, Oak Ridge National Laboratory,
Oak Ridge, Tennessee 37830

Abstract

The use of spectroscopic ellipsometry for the accurate determination of the optical properties of liquid and solid metals is discussed and illustrated with previously published data for Li and Na. New data on liquid Sn and Hg from 0.6 to 3.7 eV are presented. Liquid Sn is Drude-like. The optical properties of Hg deviate from the Drude expressions, but simultaneous measurements of reflectance and ellipsometric parameters yield consistent results with no evidence for vectorial surface effects.

MASTER

*Present address: Department of Physics, Osaka Kyoiku University,
Tennoji, Osaka, Japan.

Introduction

For many years ellipsometry has been a widely used technique in the study of surfaces. It has long been recognized, in theory, that ellipsometry is capable of yielding highly accurate values of the bulk optical properties for a clean sample as well as being sensitive to very thin surface films or to small amounts of adsorbed materials. Before the advent of ultrahigh vacuum techniques, it was difficult to produce and maintain sufficiently clean surfaces for the determination of accurate values of the bulk optical properties of a metal by ellipsometry. Because of this and the known sensitivity of ellipsometry to surface films, one of its more routine applications has been to monitor a change occurring at a surface with time (e.g., oxidation of the surface), as long as this did not proceed too rapidly. A single ellipsometric measurement was quite complex and time consuming, and extraction of the optical properties of the sample from the measured ellipsometric parameters was computationally challenging. For these reasons early ellipsometers were mostly designed for use at a single wavelength. With the development of fast automated ellipsometers and the almost universal availability of adequate computing facilities, spectroscopic ellipsometry has now become a very powerful tool, with enormous potential, for the study of metals [1-5]. Combined with present day ultrahigh vacuum techniques, spectroscopic ellipsometry can now yield accurate bulk optical properties of clean samples. In addition, simultaneous ellipsometric and reflectance measurements on the same clean sample can yield information about intrinsic properties of the surface. The application of ellipsometry to the study of thin surface films is currently expanding in scope. It is anticipated, for example, that there

will be increased use of ellipsometry in many biological and medical problems involving membranes or macromolecules on surfaces [6,7]. Interferometric ellipsometry [8], ellipsometry combined with surface electromagnetic waves [9], and the study of multilayer systems by a combination of internal and external ellipsometry [10] will all, undoubtedly, be expanded to a range of wavelengths. These spectroscopic ellipsometry techniques will each yield specific information about the surface that is probed. Different types of ellipsometric systems with their advantages and disadvantages and the accuracies attainable have been reviewed by Aspnes [1] and by Kinoshita and Yamamoto [11].

In this review we will demonstrate the necessity of employing spectroscopic ellipsometry techniques in the determination of accurate values for the optical properties of solid and liquid metals in the energy range from the infrared to the near ultraviolet. This energy range, below the volume plasmon energy for most metals, is an energy range of great interest. However, the optical conductivity is usually very high over much of this region, and thus the normal incidence reflectance is relatively insensitive to the optical properties of the metal. Reflection ellipsometry is far more sensitive, both to the optical properties of the bulk metal and to the surface conditions. Because of this sensitivity to surface conditions, early data obtained by spectroscopic ellipsometry for a particular material were not necessarily reproducible from one experimental arrangement to the next. One example is the so-called Mayer-El Naby anomaly in the optical absorption of alkali metals, first reported in 1963. It is only recently that consistent, accurate data characteristic of the clean metal have been obtained using ultrahigh vacuum reflection ellipsometry.

Optical properties have been obtained for most metals in their solid state over an extended energy range. In Section I we discuss recent studies of the optical properties of solid Li and Na, with emphasis on the accuracy attainable. Optical properties have been obtained for relatively few liquid metals and, in general, these are over very limited energy ranges. Existing data for liquid metals are discussed, and new data on liquid Sn are presented in Section II. In Section III we present new data on liquid Hg. The optical properties of liquid Hg have evoked particular interest. A consistent difference has been observed between the optical properties deduced from reflectance and from ellipsometric spectra, which has led to the proposal of various surface models. We show that no real differences are found between the optical properties deduced from reflectance and from ellipsometric measurements and that there is no evidence for any surface structure for liquid Hg. The optical constants of bulk Hg, obtained most accurately by ellipsometry, are, however, non-Drude-like and this deviation from classical behavior requires theoretical explanation.

I. Solid Li and Na

For many years interest in the alkali metals centered around anomalous structure seen by some workers in the IR to visible region of the absorption spectra. As an example, most of the experimental results for solid Na, published up to 1974, are shown in Fig. 1 in the form of the optical conductivity σ defined by $\sigma = \omega \epsilon_2 / 4\pi$, where ϵ_2 is the imaginary part of the dielectric function and ω is the angular frequency of the incident photons. All of these results were obtained using ellipsometric techniques. It was realized that, for the alkali metals in this energy region, the high values observed for reflectance make it difficult to obtain accurate values of the optical properties. This also applies for other solid and liquid metals and will be demonstrated for Hg in Section III. From the data shown in Fig. 1 for solid Na, only Smith's results [12] can be interpreted in terms of a nearly-free-electron theory and the known band structure of Na. The double-peak structure observed by Mayer and Hietel [13] cannot be explained by a simple theory and was termed anomalous. It is to be noted that even studies performed after the development of ultrahigh vacuum techniques show significantly different spectra, presumably due to such factors as the roughness, crystallinity, granularity, and contamination of the surfaces studied.

As part of a program designed to study the optical properties of liquid alkali metals, we determined the optical properties of Na and Li, between 0.6 and 3.8 eV, in the form of thick evaporated solid films [14]. The ellipsometer and experimental techniques have been described previously [14]. The samples were prepared and measured under ultrahigh vacuum conditions:

before and after evaporation, the pressure in the sample compartment was in the low 10^{-9} torr range. Measurements were made at room temperature by reflection ellipsometry through a quartz substrate at the quartz-metal interface. Our results [14] for solid Na, compared with those of Smith [12], are shown in Fig. 2. The anomalous structure reported by Mayer and Hietel was not seen: rather Smith's results were confirmed for the first time.

Among the wide variety of ellipsometric techniques, the photometric method of Conn and Eaton [15] was employed in this study to measure ψ and Δ defined by $\tan\psi = r_p/r_s$ and $\Delta = \Delta_p - \Delta_s$, respectively, where r_p and r_s are the reflectance amplitudes, and Δ_p and Δ_s are the phase changes upon reflection, of the components of the incident light with the electric vector parallel and perpendicular to the plane of incidence, respectively. In this method, by setting the polarizer at 45° , ψ is determined from the intensity ratio I_p/I_s of the p and s components of reflected light by $\tan\psi = (I_p/I_s)^{1/2}$, and Δ is determined from the axial ratio $(I_{\min}/I_{\max})^{1/2}$ of the ellipse of the reflected light by $\sin\Delta = \sin 2\xi/\sin 2\psi$, where I_{\min} and I_{\max} are the minimum and maximum intensities measured by rotating the analyzer around the axis of the reflected beam and $\tan\xi = (I_{\min}/I_{\max})^{1/2}$.

The advantage of this method is its high sensitivity in determining ψ . As has been discussed by Smith [12], if β is defined by $\psi = \frac{1}{2}\pi - \beta$, β is quite small for a highly reflecting surface for which r_p/r_s is very close to unity. In fact, using the conventional null method, in which the directly measured quantity is essentially the angle ψ , Smith [12] could not obtain reliable values of ψ from a single reflection at a

quartz-Na interface due to the relatively low sensitivity of the null method. In contrast, since the intensity ratio I_p/I_s can be written for small values of β as $I_p/I_s = \tan^2\psi \simeq 1 - 4\beta$, the present method is four times more sensitive than the null method. This method has even higher sensitivity than the modulation method developed by Jaspersen and Schnatterly [16] in which the quantity measured to determine ψ is $(I_s - I_p)/(I_s + I_p) \simeq 2\beta$. The contrast between the present method and the null method can be seen clearly in Fig. 3. The values of β measured by Smith [12] for a single reflection at a quartz-Na interface at an angle of incidence of 75° are plotted using open circles in the lower part of Fig. 3. Since no particular structure was found in these data, he had to make multiple reflection measurements, in which he actually measured the quantities 4β and 7β from four and seven reflections at quartz-Na interfaces. His data for 4β are shown in the upper part of Fig. 3 by open circles and these do exhibit a clear structure. The present data obtained from a single reflection at a 70° angle of incidence, and presented by filled circles in the figure, show a structure similar to that in Smith's 4β data. A technique similar to the present one has been used in Mayer and Hietel's study [13] on Na and in a study of solid Li by Mathewson and Myers [17].

As had been found previously by Smith [12] the experimental values of the optical conductivity of solid Na below the interband threshold are considerably larger than the Drude values given by $\sigma_D = Ne^2/m^*\omega^2\tau$, if σ_D is evaluated from the m^* deduced from the experimental ϵ_1 values, where

ϵ_1 is the real part of the dielectric function, and τ from the dc conductivity. In this expression, N is the density of free carriers, m^* is their effective mass, and τ is the relaxation time. Values of ϵ_1 , obtained by us, for solid Na are plotted in Fig. 4 as a function of λ^2 , the square of the wavelength in μm . Assuming the simple expression

$$\epsilon_1 = 1 + 4\pi N_0 \alpha - \left(\frac{\omega_a}{\omega}\right)^2$$

to hold for ϵ_1 , where N_0 is the number of atoms per unit volume, α is the ion core polarizability, and $\omega_a = (4\pi N e^2 / m^*)^{1/2}$, the values of m^*/m obtained are 1.07 in the IR and 1.08 in the visible and ultraviolet. The plasmon energy, $\hbar\omega_p$, defined by $\epsilon_1 = 0$ is 5.6 eV and $4\pi N_0 \alpha$, obtained for $\lambda^2 = 0$, is 0.1.

The available measurements of the room temperature optical conductivity for solid Li covering the energy range from the infrared to the near ultraviolet are presented in Fig. 5. The data by Inagaki et al. [14] were obtained using the same techniques as described for solid Na. Samples were deposited and measured at room temperature, with observations made at the quartz-lithium interface. Curve A by Mathewson and Myers [17] was measured for a Li film on a quartz substrate twelve hours after deposition, curve B was measured for the same film seven days after deposition, and curve C was obtained for a Li film on a sapphire substrate. In each case, Li was deposited on substrates cooled by liquid nitrogen and then measurements made at room temperature at the vacuum-Li interface. Hunderi's measurements [18] were made at room temperature at the vacuum-Li interface

on films which had been prepared by evaporation onto sapphire substrates cooled to 80°K. Myers and Sixtensson's results [19] were obtained from measurements made at room temperature at the vacuum-Li interface. The film believed to be characteristic of the BCC structure was deposited on a sapphire substrate cooled to 15°K, while that believed to be characteristic of the HCP structure was deposited on a sapphire substrate cooled to 80°K. Both samples were annealed at room temperature prior to measurements being made. Mathewson and Myers [17] stated that, of their data, curve C was most likely characteristic of the BCC structure in Li. They further assumed that changes with time indicated a change in crystalline structure of their sample. Most of the Li films studied by Inagaki et al. [14] were stable and did not change with time. For the few films that did change, increased absorption was seen in the vicinity of 2 eV, rather than the types of change in structure seen by others and indicated by Fig. 5.

It is known that Li is a difficult metal to work with. It is highly reactive and its crystalline structure is found to depend critically on the method of film preparation. As seen in Fig. 5, there is no demonstrated consistency in the experimental optical conductivity spectra obtained from ellipsometric measurements at room temperature. Assuming the threshold for interband transitions is given by the energy corresponding to the minimum in the conductivity spectrum, none of the data shown in Fig. 5 are consistent with simple band-structure calculations. Experimentally the minima in the different studies lie in the energy range from 1.4 to 2.3 eV, whereas the predicted value is ~ 3.0 eV. Possibly, broadening of the absorption edge may shift the apparent onset of absorption so

that the observed minimum for a given curve should not be interpreted in this way. However, at this time the data on Li cannot be explained in terms of simple theories based on the nearly-free-electron model of a metal.

Rasigni and Rasigni [20] have presented optical constants for Li between 0 and 10.7 eV, calculated by a Kramers-Kronig analysis of normal incidence reflectance data. The reflectance values between 0.5 and 5 eV were obtained by direct measurement on a vacuum-Li interface at 6°K, while from 5.5 to 10.7 eV they were calculated from the optical constants determined, at room temperature, by Callcott and Arakawa [21] from observations of reflectance as a function of angle of incidence at both the vacuum-Li and substrate-Li interfaces. Their Kramers-Kronig analysis was normalized to Inagaki et al. [14] from 2 to 3 eV and to Callcott and Arakawa [21] from 6.5 to 9 eV. Values of the refractive index, n , and extinction coefficient, k , obtained by Rasigni and Rasigni are shown in Fig. 6 compared with the same quantities obtained by Inagaki et al. and Callcott and Arakawa. It is seen that, even with the normalization of the Kramers-Kronig analysis in the 2 to 3 eV region, there are significant differences between the optical constants obtained from reflectance and from ellipsometric measurements in the infrared and visible regions.

Li, with its low atomic number and relatively simple atomic structure, is of great theoretical interest. Further experimental studies of the optical properties of solid, and liquid, Li under controlled conditions, coupled with surface characterizations, are required.

II. Liquid Metals

Liquid metal samples in equilibrium with their environment are free of macroscopic surface roughness effects. In addition, geometrical factors involving granularity and different crystalline forms of the metal which can affect the values obtained for the optical properties of solid metals are not encountered for liquid metals. Under ultrahigh vacuum conditions, the surface can also be obtained free of contamination. Thus, in principle, it should be easier to obtain accurate values of the bulk optical properties of a metal in its liquid state than in its solid state. Experimentally, the temperatures required to melt most metals make optical measurements under ultrahigh vacuum conditions difficult to perform. Consequently there is a relative sparsity of optical data on liquid metals other than Hg.

Existing optical data on liquid metals obtained by ellipsometric techniques are mainly attributable to Kent [22] (Cd, Sn, Pb, Bi), Hodgson [23] (Cu, Ge, Ag, Cd, In, Sn, Sb, Te, Hg, Pb, Bi), Lelyuk¹ et al. [24] (Ga, Hg), Mayer and Hietel [13] (Na, K, Rb, Cs), Smith [25] (Cd, Hg, Pb, Bi), Miller [26] (Al, Fe, Co, Ni, Cu, Ag, Au), Comins [27] (Al, Cu, Ga, Sn, Au, Hg, Pb, Bi), and Inagaki et al. [28] (Na). Measurements of reflectance have been employed by Schulz [29] (Ga, Hg), and Wilson and Rice [30] (In, Hg, Bi). In addition there are several other determinations of the optical properties of liquid Hg which will be referenced in Section III. Many of these measurements on liquid metals are over a very limited energy range. Exceptions are the reflectance spectra obtained by Wilson and Rice from 2 to 20 eV. It has been found that the optical properties

of many liquid metals can be explained in terms of the simple Drude theory, at least over limited energy ranges, as long as n^2 (or N^* , an effective density of free carriers) and τ are treated as adjustable parameters, i.e., the optical properties of many of the liquid metals which have been studied experimentally can be explained in terms of a nearly-free-electron theory. A notable exception is liquid Hg, which will be discussed in Section III. In fact, simple metals, having weak electron-ion interactions (e.g., Na, Al, etc.) are described by a nearly-free-electron theory and can be expected to obey the Drude formulae, whereas for metals where the scattering interaction is strong (e.g., transition and rare earth metals, divalent metals, Be, Hg, Ba, etc.) there are more uncertainties in the theory and more probability of non-Drude-like behavior [31]. In addition, band gaps characteristic of long-range order are destroyed by melting, and it is to be expected that the corresponding structures would be removed from the energy spectrum of the liquid metal [31,32]. For several metals, structures in the optical properties of the solid associated with transitions from the conduction band to states above the Fermi level have not been observed in the spectrum for the liquid. On the other hand, we will show that structure for liquid Na appears at the same energy as structure for solid Na. When transitions in the solid metal are from the d-bands to the Fermi level, structure has been found to persist in the spectrum for the liquid [26,30]. Thus, as might be expected, some short-range order exists in liquid metals which is similar to that which exists in the corresponding solid. In fact, from theoretical and experimental arguments, based principally on correlations between nuclear magnetic resonance measurements and electronic structure, Knight and Berger [33] concluded that a liquid metal possesses a band structure which is very like that of its solid,

provided the short-range structure is not altered during melting. Although the long-range order, which is normally associated with the existence of Brillouin zones, is destroyed on melting, they present a model which can lead to a band structure in some liquid metals.

The optical conductivity spectra for solid and liquid Na can be examined from the point of view of the above arguments. Our data for solid Na [14] have been presented in Fig. 2, while our data for liquid Na [28], obtained using essentially the same techniques on free surfaces of Na at 120°C, are shown in Fig. 7. In contrast to the case of solid Na, the absorption properties in liquid Na below 2.2 eV can be described well by the simple Drude model of free-carrier absorption. Above 2.2 eV, absorption is greater than predicted by the simple Drude model. Although Smith [34] has shown theoretically that the interband transition in solid Na, seen in the region of 3 eV in Fig. 2, should not persist into the liquid phase, Knight and Berger [33] suggest, from observations of nuclear magnetic resonance line shifts in liquid and solid alkali metals, that the electronic structures of the respective solids and liquids are the same. This would justify our interpretation [23] of the structure seen in the optical conductivity of liquid sodium above about 2.2 eV as being due to a liquid analog of the interband absorption seen in the spectrum for the solid. On the other hand, Helman and Baltensperger [35] claim that this discrepancy between our experimental results and the simple Drude formula does not arise from an interband transition but from the fact that the relaxation time τ is frequency dependent when the electron-ion interaction in the liquid metal is properly taken into account.

We have recently obtained the optical properties of liquid Sn [36] at 261°C from ellipsometric measurements for photon energies between 0.62 and 3.7 eV. Measurements were made at a vacuum-liquid Sn interface after contaminants were removed from the liquid surface using a stainless steel scraper. The real and imaginary parts, ϵ_1 and ϵ_2 , of the dielectric function are shown in Fig. 8 together with the values obtained previously by Kent [22], Hodgson [23] and Comins [27], and the corresponding Drude curves. Figure 9 shows the variation of $(1 - \epsilon_1)^{-1}$ with λ^{-2} for our values of ϵ_1 for liquid Sn. This curve is of interest since all data from the infrared through the ultraviolet fall on a single straight line yielding a single value of m^* from the slope. This is contrary to the results for other metals in the solid and liquid phases (compare Fig. 4) where different values of m^* are obtained in the infrared and in the visible and ultraviolet regions. It is seen that liquid Sn behaves like a nearly-free-electron metal over the full range of the experimental measurements. There is no evidence of the interband transitions seen in solid Sn at 1.2 eV and ~3 eV [37]. A value of $m^*/m = 0.98 \pm 0.05$ was obtained from the slope of Fig. 9, compared with ~3.0 for solid Sn [36]. The sum rule

$$\int_0^{\infty} \sigma(\omega) d\omega = \frac{\pi}{2} \left(\frac{N_T}{m} \right) e^2,$$

where N_T is the total electron density, requires that if some interband transitions of various electrons disappear on melting, then the value of m^* representing intraband transitions will decrease. This is true for Sn [32].

The measurement of the optical properties of liquid metals over an extended energy range, from the infrared to the vacuum ultraviolet, deserves more attention. In particular, the observation of the optical properties of a metal in both the solid and liquid states obtained in the same experiment under ultrahigh vacuum conditions by spectroscopic ellipsometry would be of great interest. Accurate measurements, on well-characterized surfaces, would yield information of relevance to theories of order-disorder on going from the solid to the liquid [38].

III. Liquid Hg

Mercury would appear, at first, to be an easy place to start in a study of the optical properties of liquid metals. It is easy to handle, stable, and liquid at room temperature. Furthermore, it is relatively easy to obtain a clean Hg surface. In 1957, Schulz [29] surveyed the literature and on the basis that there were many measurements available in the visible, some in the ultraviolet, and a few in the infrared for liquid Hg, and only the measurements by Kent [22] at three wavelengths in the visible available for other liquid metals, came to the conclusion that "If the goal is to find a metal which is most likely to follow the Drude theory over a long wavelength range, the evidence points toward liquid Hg as being the most promising metal." Schulz, from his reflectance measurements, then presented a strong case for the validity of the Drude theory in liquid Hg. Since then a consistent difference has been observed between the optical properties deduced from reflectance and from ellipsometric spectra. To reconcile the two sets of results, Bloch and Rice [39] proposed a surface transition zone. From ellipsometric and reflectance measurements made simultaneously on the same samples, Crozier and Murphy [40] concluded that such a model, coupled with vectorial optical properties for the liquid Hg, was consistent with their data. Guidotti and Rice [41] probed the liquid Hg surface directly using an attenuated total reflection method to excite surface plasmons and expressed the vectorial effect in terms of a conductivity in the surface layer which is both anisotropic and larger than the value in the bulk. We have recently measured simultaneously the absolute reflectances R_s and R_p and the

ellipsometric parameter Δ for liquid Hg over the energy range from 0.6 to 3.7 eV [42]. No systematic differences were found between the optical properties deduced from reflectance and from ellipsometry, in contrast to the results of Crozier and Murphy. In this Section we present an analysis to demonstrate that neither the previously existing nor our new ellipsometric data show evidence for any intrinsic surface structure in liquid Hg. By use of a Kramers-Kronig analysis it is then shown that it is the optical properties obtained from ellipsometric measurements that are representative of liquid Hg. Finally, it is shown that there is no real conflict with the optical properties deduced from reflectance data as there are large inherent uncertainties associated with this method when used for metals in the infrared to near ultraviolet energy region.

Liquid Hg, cleaned by the overflow method previously used by Hodgson [23], was brought into contact with a strain-free quartz prism. Measurements were made on this system at atmospheric pressure. At all times during the measurements the surfaces could be inspected and were found free of visible contamination. The experimental method of obtaining R_p , R_s , and Δ was almost identical to that used by Crozier and Murphy [40]. The azimuth setting of the polarizer was fixed at 45° to the plane of incidence. Two sets of intensities $I(0^\circ)$ and $I(90^\circ)$, and $I(45^\circ)$ and $I(135^\circ)$ were measured for reflection from the quartz-liquid Hg interface, where $I(A^\circ)$ is the intensity measured with the analyzer setting at A° to the plane of incidence. The liquid Hg was then removed and the values of the intensities $I_0(0^\circ)$ and $I_0(90^\circ)$ recorded for total internal reflection at the quartz-air interface. The angle of incidence was determined to be 60.52° from the value of Δ obtained from these total reflection measurements. R_p and R_s were given by $R_p = I(0^\circ)/I_0(0^\circ)$ and $R_s = I(90^\circ)/I_0(90^\circ)$,

respectively, and Δ was determined from [40] $\cos\Delta = -\cos 2\xi/\sin 2\psi$, where $\tan\xi = [I(45^\circ)/I(135^\circ)]^{1/2}$ and $\tan\psi = [I(0^\circ)/I(90^\circ)]^{1/2}$. The parameter ψ was actually obtained from $\tan\psi = [R_p/R_s]^{1/2}$.

The dielectric functions ϵ_1 and ϵ_2 were calculated from the measured ellipsometric parameters ψ and Δ . The values obtained for ϵ_2 , in the form of the optical conductivity σ , are shown in Fig. 10 and those for ϵ_1 in Fig. 11. Also shown are previous values appearing in the literature [23, 25, 27, 40, 43-47], all of which have apparently been obtained from ψ and Δ under the same assumption of no surface effects. The notation $n_0 = 1.00$ indicates the data were obtained at a vacuum (or inert gas)-liquid Hg interface, $n_0 = 1.42$ at a cyclohexane ($n_0 = 1.4198$)-liquid Hg interface, and $n_0 = n_Q$ at a quartz-liquid Hg interface. The measurements of Smith and Stromberg [47] at 2.27 eV also included $n_0 = 1.5084$ (benzene) and $n_0 = 1.3344$ (water). No differences were found in their values of ϵ_1 and ϵ_2 within their experimental accuracy of four significant figures. The Drude variations of σ and ϵ_1 were calculated from

$$\tilde{\epsilon}_D = 1 - \frac{4\pi N \sigma_0}{(\tau/h)E^2 + iE}$$

where τ , the relaxation time for free carriers, was determined [44] from $\tau = (m/Ne^2)\sigma_0$ using the d.c. conductivity $\sigma_0 = 9.387 \times 10^{15} \text{ sec}^{-1}$ and the density of free carriers $N = 8.158 \times 10^{22} \text{ cm}^{-3}$ for liquid Hg at 20°C. An imperfect glass-liquid Hg contact [43, 44] apparently caused the considerable difference between the results of Lelyuk et al. [24] and those shown in Figs. 10

and 11. The experimental data, obtained in the various studies represented, are consistent with each other, with no systematic correlations of σ or ϵ_1 with the value of n_0 . The dashed curves indicate the probable upper and lower limits of the observed quantities. It is seen that the optical properties of liquid Hg, as observed by ellipsometric measurements, are not represented by the Drude nearly-free-electron model.

The lack of any demonstrated differences in the experimental values of σ and ϵ_1 for different values of n_0 is strong evidence for the absence of any surface structure in liquid Hg. If the surface models [39,41] proposed for liquid Hg were applicable, then measurements made with different materials (i.e., different n_0 values) in contact with the liquid Hg, and analyzed assuming no surface structure, would give apparent optical properties for liquid Hg which varied as a function of the value of n_0 .

Consider liquid Hg [47], with $\epsilon = -18.46 + i13.50$, covered with a 10\AA thick transparent layer of refractive index $n_1 = 1.45$ as shown in Fig. 12. As defined by Burge and Bennett [48], we call the dielectric function ϵ , calculated from the measured ellipsometric parameters ψ and Δ for a real surface under the assumptions that the surface is smooth, homogeneous, and isotropic, the pseudodielectric function. If surface structure is present on the real surface, then the pseudodielectric function will, in general, be a function of ϕ and n_0 , the angle of incidence and the refractive index of the ambient medium, respectively. The calculated pseudodielectric functions for the chosen example at a photon energy of 2.27 eV, are shown as functions of ϕ and n_0 in Fig. 12. For $\phi = 70^\circ$, the variations of ϵ_1 and ϵ_2 with n_0 are large enough to indicate experimentally the existence of the surface structure.

Most ellipsometric data are taken at an angle of incidence in the region of 70° ($\pm 10^\circ$) and thus, if there is a surface layer on liquid Hg with properties resembling those shown in Fig. 12, it should show up as systematic differences in σ and ϵ_1 with n_0 in Figs. 10 and 11. Other reasonable values of n_1 and thickness of the surface layer lead to the same conclusion. Thus lack of systematic variations in σ and ϵ_1 with the value of n_0 implies that there is no surface layer or surface inhomogeneity on liquid Hg. A similar analysis [42] rules out any anisotropy in the optical properties of liquid Hg in the vicinity of its surface.

The pseudodielectric function $\epsilon(n_0, \phi)$ can be used in several other tests for surface structure. For example, a value of $\epsilon(n_0, \phi)$ obtained for a real surface at a given photon energy can be used to calculate the anticipated variation of the reflectance at that energy as a function of the refractive index of the ambient medium, n_0' , and the angle of incidence ϕ' . This quantity, $R_{\text{ant}}(n_0', \phi')$ can then be compared with the experimentally observed quantity, $R_{\text{exp}}(n_0', \phi')$. Assuming the system shown in Fig. 12 with $n_0 = 1$ and $\phi = 70^\circ$, the quantities $R_{\text{ant}}(n_0', \phi')$ and $R_{\text{exp}}(n_0', \phi')$ have been calculated. The difference $\delta R = R_{\text{ant}}(n_0', \phi') - R_{\text{exp}}(n_0', \phi')$ has been plotted in Fig. 13 which shows δR_p and δR_s as functions of n_0' and ϕ' . $\delta\psi$ and $\delta\Delta$, calculated for the same system, are also shown in Fig. 13. It is seen that δR_p or $\delta\Delta$, for $n_0' \neq n_0$ and large values of ϕ' are large enough to be detected, if surface structure exists.

The present measurements of R_p on liquid Hg were used to perform a δR_p -check. For this purpose the available pseudodielectric functions obtained with $n_0 = 1$ at each energy (Figs. 10 and 11) were used to calculate the anticipated

value of R_p for $n_o' = n_Q$ and $\phi' = 60.52^\circ$, i.e., the actual experimental conditions of our measurement of R_p . The anticipated and measured values of R_p for our present studies on liquid Hg are shown in the top part of Fig. 14. Also shown in the lower part of Fig. 14 is a similar comparison for the measurements of Crozier and Murphy [40]. In both studies, values of R_p obtained by direct measurement at the quartz-liquid Hg interface and the corresponding calculated quantity both show a systematic deviation from the Drude values, but are in good agreement with each other.

Further tests for the detection of surface structure from ellipsometric measurements involve searching for inconsistencies in the values of R_p , R_s , and Δ measured simultaneously at a given interface. One method involves comparing one of these measured quantities with its value as calculated from the other two. Another method involves calculating the optical constants from three different pairs of the measured quantities. These tests have been described previously [42]; none show any evidence for surface structures in liquid Hg.

The apparent Drude optical properties of liquid Hg, which have been extracted from two or more reflectance measurements at a given energy, and which have been thought to be in conflict with the ellipsometric measurements, can be shown [42] to be unreliable because of the large uncertainties involved in the reflectance measurements relative to the accuracy necessary to obtain reliable optical properties in this energy range. Figure 15 shows plots in the ϵ_1 - ϵ_2 plane of calculated equireflectance curves. For each curve the type of reflectance measurement is specified by a subscript (\bar{R} = reflectance at $\phi = 45^\circ$ for unpolarized light), the value of the ambient

refractive index is given, and the stated value of the reflectance has been obtained from the Drude values of ϵ_1 and ϵ_2 for liquid Hg at 2.27 eV. Also indicated on each curve is an error bar of length $2R_{\text{err}}$ which corresponds to a typical range of the experimental uncertainty reported in the literature. This error bar specifies a path $2R_{\text{err}}$ wide centered on the equireflectance curve. When two experimental values of reflectance, such as $R_N(n_0 = 1.0)$ and $R_N(n_0 = 1.4)$, at 2.27 eV are used to determine ϵ_1 and ϵ_2 for liquid Hg, the values obtained from the intersection of the equireflectance curves will lie within the overlap region of the corresponding paths. Because the equireflectance curves are almost parallel, the region of overlap for any two of the types of reflectance measurements shown in Fig. 15 extends from the top of the graph to beyond the bottom. This demonstrates that optical properties obtained from reflectance measurements have large associated errors: in the case of Fig. 15, depending on the pair of reflectances, this error may be ~ 60 to $\sim 100\%$. At lower photon energies the uncertainties associated with optical properties determined by this method are even larger. Bloch and Rice [39] report R_N for various values of n_0 while Mueller [49] reports R_N and R_S at $\phi = 45^\circ$ for liquid Hg in contact with sapphire. In both cases, they contend that since they observe values of reflectance consistent with the Drude values of ϵ_1 and ϵ_2 that this proves the validity of the Drude values. We have shown that there is a very large uncertainty in the optical properties when they are determined from reflectance measurements, and that observing "Drude" reflectances does not necessarily imply Drude values of the optical properties. In fact, we demonstrate in

Fig. 15 that the reflectances measured by Bloch and Rice and by Mueller are not inconsistent with the values of ϵ_1 and ϵ_2 obtained by ellipsometry for liquid Hg at 2.27 eV. These values, using the same notation as in Fig. 10, are shown in Fig. 15 together with a rectangle of dashed-lines indicating the probable upper and lower limits. In order to determine the optical constants by reflectance measurements with accuracy comparable to that of the ellipsometric results, reflectances would have to be measured ten to a hundred times more accurately than in the experiments so far reported in the literature. In fact, the high correlation between the determination of the optical properties from reflectance measurements and the consistency of those properties with the Drude theory seems to stem from the a priori assumption, in some cases, of the validity of Drude theory.

Of the reported reflectance measurements, only those of Schulz [29] do not fall in the above category. Schulz obtained values of the optical properties from measurements of \bar{R} and θ , the phase change for reflectance at normal incidence. In a ϵ_1 - ϵ_2 plane, equi- \bar{R} and equi- θ curves cross nearly at right angles and experimental errors introduce only small errors into the values determined for ϵ_1 and ϵ_2 . Similar considerations apply to equi- ψ and equi- Δ curves which are employed in the ellipsometric determination of the optical properties. Schulz's experiments appear to have been performed to a high standard of experimental accuracy and examination of his published papers does not reveal any apparent reason to doubt the "Drude" values which he obtained [42]. However, detailed Kramers-Kronig analyses, over a wide energy range [42], show that Drude optical properties are not possible for liquid Hg, whereas the optical properties

obtained from ellipsometric measurements are internally consistent with the available data on liquid Hg above the limit of the ellipsometric measurements at ~ 5 eV.

The Kramers-Kronig relation used was that for the phase change on reflection at normal incidence

$$\theta(E) = -\frac{1}{\pi} \int_0^{\infty} \frac{E' \ln R_N(E')}{(E')^2 - E^2} dE'$$

If $R_N(E')$ and $\theta(E)$ are calculated from the pseudodielectric functions obtained from ellipsometric measurements on real surfaces on the assumption that there is no surface structure, this Kramers-Kronig relation would appear to break down in the presence of surface structure. However, this test for the presence of surface structure cannot be applied as experimental values of the pseudodielectric function are not available over the whole energy spectrum. We can use this relation to demonstrate that the Drude values of θ obtained by Schulz are highly unlikely, whereas the optical properties determined from ellipsometric measurements are probably correct.

The measured values of the normal incidence reflectance, R_N , obtained by Wilson and Rice [30] from 2 to 20 eV are shown in Fig. 16. Wilson and Rice analyzed these data through the Kramers-Kronig relation by assuming the Drude form for R_N below 2 eV and an analytic extrapolation of the measured R_N to energies above 20 eV. They obtained values of the optical properties from 2 to 20 eV which are quite close to the Drude values in the region below 4 eV. This analysis was somewhat circuitous, however, since

the extrapolation of R_N to high energies was chosen to give the Drude value of θ at 2.0 eV. In an attempt to obtain a more realistic extrapolation of R_N above 20 eV, in the absence of optical data for either liquid or solid Hg, we have used the optical data available in the literature [50] up to 900 eV for two materials with atomic numbers close to that of Hg ($Z = 80$) to estimate values of R_N for Hg. From solid Au ($Z = 79$),

$$R_{N,Hg} = (D_{Hg}/D_{Au})^2 R_{N,Au} = 0.476 R_{N,Au}$$

where D_{Hg} and D_{Au} are the atomic densities in liquid Hg and solid Au, respectively. Similarly, from solid Bi ($Z = 83$),

$$R_{N,Hg} = (D_{Hg}/D_{Bi})^2 R_{N,Bi} = 2.077 R_{N,Bi} .$$

These estimated values of R_N are shown in Fig. 16 and appear to agree reasonably well with each other above ~ 50 eV. This agreement demonstrates that this is a reasonable method of determining R_N for high Z materials at high enough energies, hence removing a major part of the uncertainty involved in the extrapolations used by Wilson and Rice. Above 900 eV we extrapolated R_N according to an E^{-4} dependence.

The results of our Kramers-Kronig analyses are demonstrated in Fig. 17 in the form of the difference between $\theta(E)/E$ calculated from the R_N values shown in Fig. 16 and the corresponding Drude values. The two solid lines were obtained, in this way, from the R_N values of Wilson and Rice [30] from 2 to 20 eV in combination with the R_N values of solid Au and solid Bi, respectively. The two dashed lines were obtained from R_N calculated from optical properties obtained from ellipsometric measurements

from 0.2 to 4 eV in combination with the R_N values of Wilson and Rice from 5 to 20 eV and the R_N values of Au and Bi, respectively. Also shown in Fig. 17 are $\theta(E)/E - \theta_D(E)/E$ calculated directly from the optical properties of liquid Hg obtained from ellipsometric measurements as summarized in Figs. 10 and 11 and from the "Drude values" of $\theta(E)$ obtained by Schulz [29]. It is seen that the calculated values of $\theta(E)/E - \theta_D(E)/E$ obtained from ellipsometric measurements lie essentially within the dashed curves. Thus, the variations with energy of the plotted function of θ obtained through a Kramers-Kronig analysis are consistent with the ellipsometric optical properties of liquid Hg. Just as the estimated R_N values using the Au and Bi data between 20 and 50 eV obviously set upper and lower limits, respectively, on the R_N for liquid Hg in this energy range, the dashed curves in Fig. 17 obtained from ellipsometric R_N , set reasonable limits on the ellipsometric data. By a proper choice of R_N between 20 and 50 eV it is obviously possible to reproduce the ellipsometric values of θ from the ellipsometric values of R_N using the Kramers-Kronig relation for $\theta(E)$.

On the other hand, the "Drude values" of Schulz are inconsistent with a Kramers-Kronig analysis employing any reasonable extrapolation. One possible explanation for this discrepancy is that the Ag film which Schulz deposited on a mica film in order to make a good mica-Hg contact did not dissolve away completely as expected.

In conclusion, it has been shown that the optical properties obtained from ellipsometric measurements are representative of bulk liquid Hg. No evidence is seen in any of the experimental data on liquid Hg to indicate

existence of surface structure or anomalous surface properties. The optical properties of liquid Hg are not Drude-like. The only known attempt to explain deviations from the simple Drude theory in liquid Hg is due to Smith [51]. Previously, with undue emphasis given to reflectance measurements and the expectation of Drude behavior, the deviations shown by ellipsometric measurements were suspect. Since it has now been established that the ellipsometric values are probably correct, there is a need for new theoretical efforts to explain the non-Drude behavior of liquid Hg.

Acknowledgment

Research sponsored by the Office of Health and Environmental Research, U. S. Department of Energy, under contract W-7405-eng-26 with the Union Carbide Corporation.

References

1. D. E. Aspnes, in: Optical Properties of Solids; New Developments, Ed. B. G. Seraphin (North-Holland, Amsterdam, 1976) p. 799.
2. R. M. A. Azzam and N. M. Bashara, Ellipsometry and Polarized Light (North-Holland, Amsterdam, 1977).
3. Ellipsometry in the Measurement of Surfaces and Thin Films, Eds. E. Passaglia, R. R. Stromberg and J. Kruger, NBS Misc. Publ. 256 (U.S. GPO, Washington, D.C., 1964).
4. Recent Developments in Ellipsometry, Eds. N. M. Bashara, A. B. Buckman and A. C. Hall (North-Holland, Amsterdam, 1969).
5. Third International Conference on Ellipsometry, Eds. N. M. Bashara and R. M. A. Azzam (North-Holland, Amsterdam, 1976).
6. A. Rothen, in: Progress in Surface and Membrane Science, Vol. 8, Eds. D. A. Cadenhead, J. F. Danielli and M. D. Rosenberg (Academic Press, New York, 1974) p. 81.
7. G. T. Ayoub and N. M. Bashara, J. Opt. Soc. Am. 68 (1978) 978.
8. H. F. Hazebroek and A. A. Holscher, Proc. 6th Internl. Vacuum Congr. 1974. Japan J. Appl. Phys. Suppl. 2, Pt. 1 (1974) 673.
9. F. Abelès, Surf. Sci. 56 (1976) 237.
10. E. C. Chan and J. P. Marton, J. Appl. Phys. 43 (1972) 4027.
11. K. Kinoshita and M. Yamamoto, Thin Solid Films 34 (1976) 283.
12. N. V. Smith, Phys. Rev. Lett. 21 (1968) 96; Phys. Rev. 183 (1969) 634.
13. H. Mayer and B. Hietel, Optical Properties and Electronic Structure of Metals and Alloys, Ed. F. Abelès (North-Holland, Amsterdam, 1966) p. 47.

14. T. Inagaki, L. C. Emerson, E. T. Arakawa and M. W. Williams, Phys. Rev. B13 (1976) 2305.
15. G. K. T. Conn and G. K. Eaton, J. Opt. Soc. Am. 44 (1954) 546.
16. S. N. Jasperson and S. E. Schnatterly, Rev. Sci. Instrum. 40 (1969) 761.
17. A. G. Mathewson and H. P. Myers, Philos. Mag. 25 (1972) 853.
18. O. Hunderi, Surf. Sci. 57 (1976) 451.
19. H. P. Myers and P. Sixtensson, J. Phys. F: Metal Phys. 6 (1976) 2023.
20. M. Rasigni and G. Rasigni, J. Opt. Soc. Am. 67 (1977) 54.
21. T. A. Callcott and E. T. Arakawa, J. Opt. Soc. Am. 64 (1974) 839.
22. C. V. Kent, Phys. Rev. 14 (1919) 459.
23. J. N. Hodgson, Phil. Mag. 4 (1959) 183; 5 (1960) 272; 6 (1961) 509; 7 (1962) 229; 8 (1963) 735.
24. L. G. Lelyuk, I. N. ShRlyarevskii and R. G. Yarovaya, Opt. Spectrosc. 16 (1964) 263.
25. N. V. Smith, Adv. Phys. 16 (1967) 629.
26. J. C. Miller, Phil. Mag. 20 (1969) 1115.
27. N. R. Comins, Phil. Mag. 25 (1972) 817.
28. T. Inagaki, E. T. Arakawa, R. D. Birkoff and M. W. Williams, Phys. Rev. B13 (1976) 5610.
29. L. G. Schulz, Adv. Phys. 6 (1957) 102.
30. E. G. Wilson and S. A. Rice, Phys. Rev. 145 (1966) 55.
31. N. H. March, Can. J. Chem. 55 (1977) 2165.
32. N. E. Cusack, in: The Properties of Liquid Metals, Ed. S. Takeuchi (John Wiley, New York, 1973) p. 157.
33. W. D. Knight and A. G. Berger, Ann. Phys. 8 (1959) 173.
34. N. V. Smith, Phys. Rev. 163 (1967) 552.

35. J. S. Helman and W. Baltensperger, Phys. Rev. B15 (1977) 4109.
36. J. P. Petrakian, A. R. Cathers, J. E. Parks, R. A. MacRae, T. A. Callcott and E. T. Arakawa, Submitted to Phys. Rev.
37. R. A. MacRae, E. T. Arakawa and M. W. Williams, Phys. Rev. 162 (1967) 615.
38. T. E. Faber, Introduction to the Theory of Liquid Metals (Cambridge University Press, Cambridge, 1972).
39. A. N. Bloch and S. A. Rice, Phys. Rev. 185 (1969) 933.
40. E. D. Crozier and E. Murphy, Can. J. Phys. 50 (1972) 1914.
41. D. Guidotti and S. A. Rice, Phys. Rev. B15 (1977) 3796.
42. T. Inagaki, E. T. Arakawa and M. W. Williams, Submitted to Phys. Rev.
43. T. Smith, J. Opt. Soc. Am. 57 (1967) 1207.
44. T. E. Faber and N. V. Smith, J. Opt. Soc. Am. 58 (1968) 102.
45. G. Busch and J. Guggenheim, Helv. Phys. Acta 41 (1968) 401.
46. W. J. Choyke, S. H. Vosko and T. W. O'Keefe, Solid State Commun. 9 (1971) 361.
47. L. E. Smith and R. R. Stromberg, J. Opt. Soc. Am. 56 (1966) 1539.
48. D. K. Burge and H. E. Bennett, J. Opt. Soc. Am. 54 (1964) 1428.
49. W. E. Mueller, J. Opt. Soc. Am. 59 (1969) 1246.
50. H. -J. Hagemann, W. Gudat and C. Kunz, Report DESY SR-74/7 (1974).
51. N. V. Smith, Phys. Lett. A26 (1968) 126.

Figure Captions

1. Optical conductivity vs incident photon energy of solid Na at room temperature. References to the data shown are given in Ref. 14.
2. Optical conductivity of solid Na obtained by Inagaki et al. [14] and Smith [12].
3. Values of β defined by $\psi = 45^\circ - \beta$ for a quartz-Na interface. The lower open circles are Smith's data [12] obtained by the null method for a single reflection at an incidence angle of 75° and the upper open circles are 4β obtained from four reflections. The filled circles are the data of Inagaki et al. [14] obtained by the photometric method for a single reflection at an incidence angle of 70° .
4. Real part of the dielectric constant of solid Na [14].
5. Optical conductivity vs incident photon energy of solid Li at room temperature.
6. Optical constants of solid Li obtained by Rassigni and Rassigni [20], Callcott and Arakawa [21] and Inagaki et al. [14].
7. Optical conductivity vs incident photon energy of liquid Na obtained by Inagaki et al. [28] and Mayer and Hietel [13].
8. Dielectric functions of liquid Sn vs incident photon energy. Drude curves for Hodgson's data and for our recent results have been calculated using parameters quoted in Ref. 36.
9. The plot of $(1 - \epsilon_1)^{-1}$ vs λ^{-2} for liquid Sn at 261°C , with λ in μm .
10. Optical conductivity vs incident photon energy of liquid Hg at room temperature. All values were obtained from ellipsometric measurements, as explained in the text. The dashed lines indicate the probable upper and lower limits of the observed conductivities.

11. Values of ϵ_1 vs incident photon energy for liquid Hg obtained from ellipsometric measurements. The different symbols refer to the references indicated in Fig. 10.
12. The pseudodielectric functions ϵ_1 and ϵ_2 obtained at 2.27 eV for liquid Hg covered with a 10 Å thick transparent layer of refractive index 1.45 as functions of the angle of incidence ϕ and the refractive index, n_0 , of the ambient medium. The dielectric constants assumed for Hg are from Smith and Stromberg [47].
13. Differences between the anticipated and experimental values of R_p , R_s , ψ , and Δ as functions of n_0 and ϕ for the system shown in Fig. 12. The anticipated values were obtained from the pseudodielectric function $\epsilon(n_0 = 1, \phi = 70^\circ)$.
14. Values of R_p measured at a quartz-liquid Hg interface compared with those anticipated from the values of the dielectric function measured at a free Hg surface.
15. Equireflectance curves R_N , \bar{R} , and R_s presented in the $\epsilon_1 - \epsilon_2$ plane. The reflectance values are those corresponding to the Drude values of the optical properties of liquid Hg at 2.27 eV. The type of reflectance and the refractive index, n_0 , of the ambient medium are indicated. The values of ϵ_1 and ϵ_2 obtained from ellipsometric measurements at 2.27 eV are shown using the same symbols as in Fig. 10. The dashed-line rectangle corresponds to the probable upper and lower limits of the ellipsometric data as indicated in Figs. 10 and 11.
16. The R_N measured by Wilson and Rice [30] at a vacuum-liquid Hg interface combined with values of R_N calculated from the experimental optical properties of solid Au and Bi [50].
17. The phase shift on reflection $\theta(E)$ divided by the photon energy E relative to the Drude values calculated from a Kramers-Kronig analysis of R_N for the vacuum-liquid Hg interface and from the dielectric function ϵ .

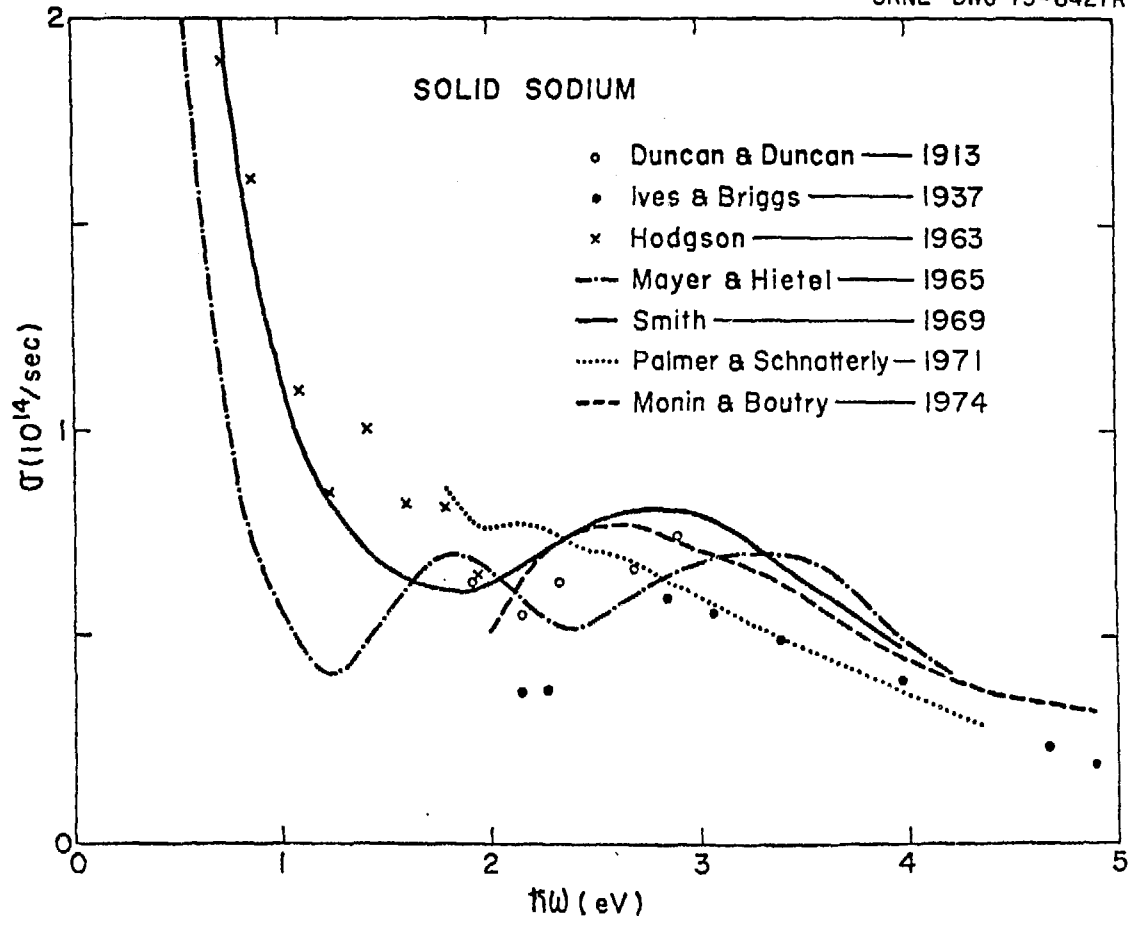


Figure 1

ORNL-DWG 75-6430R

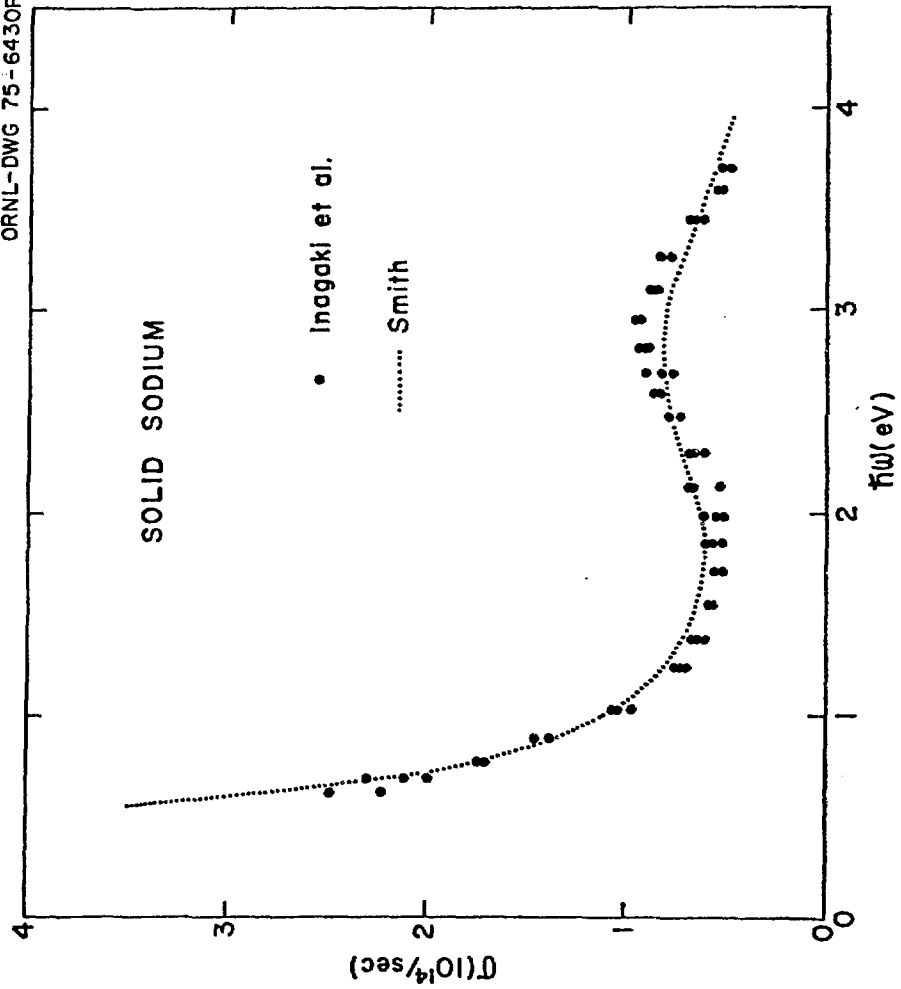


Figure 2

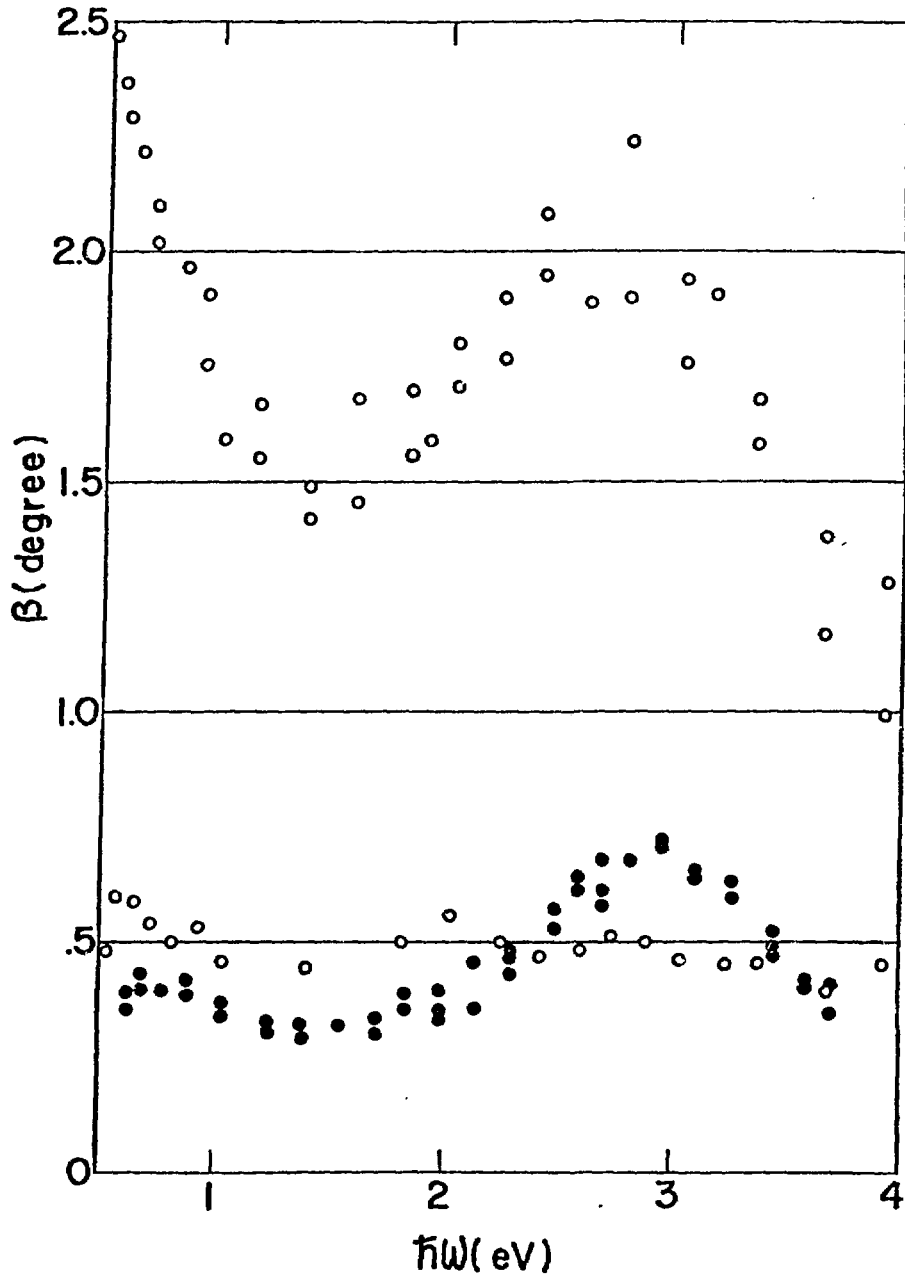


Figure 3

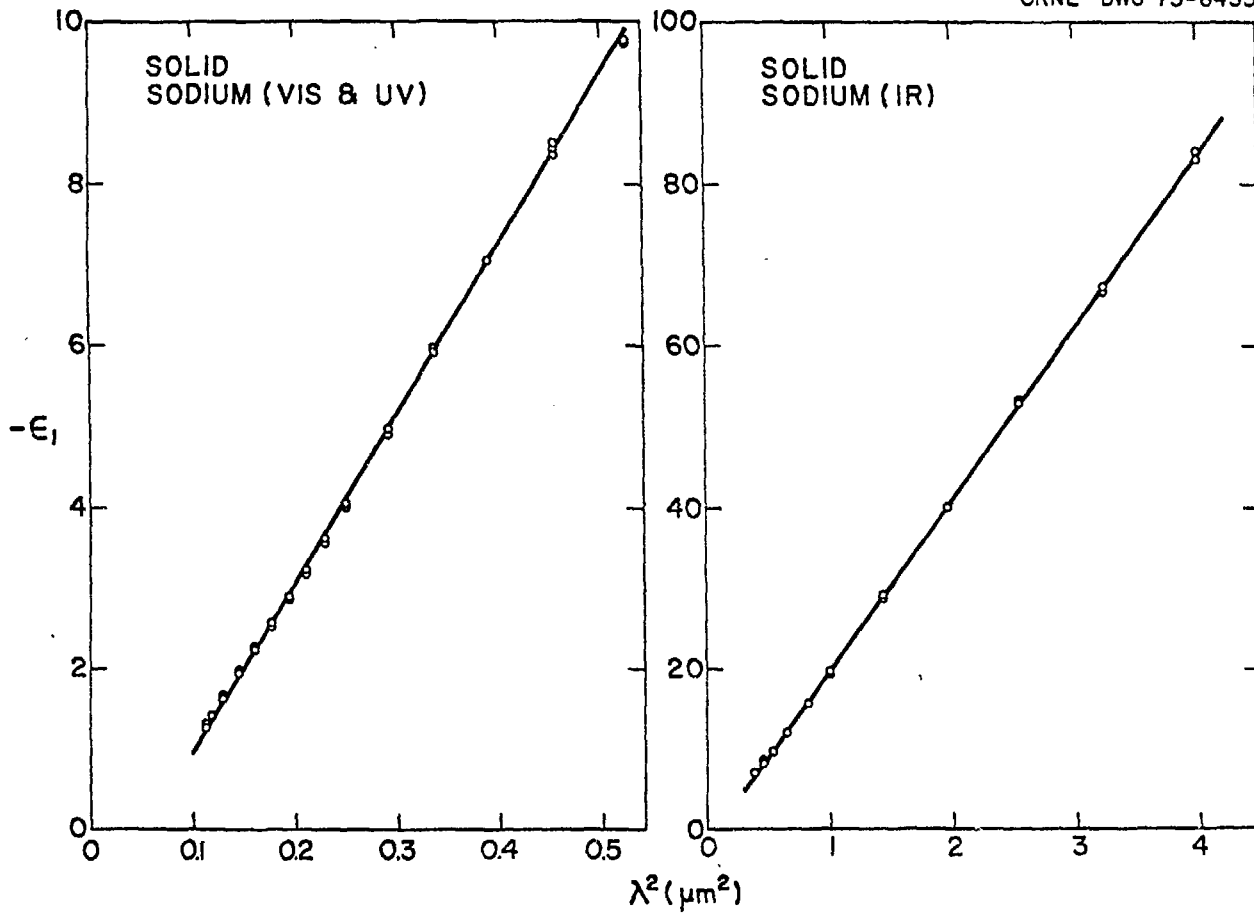


Figure 4

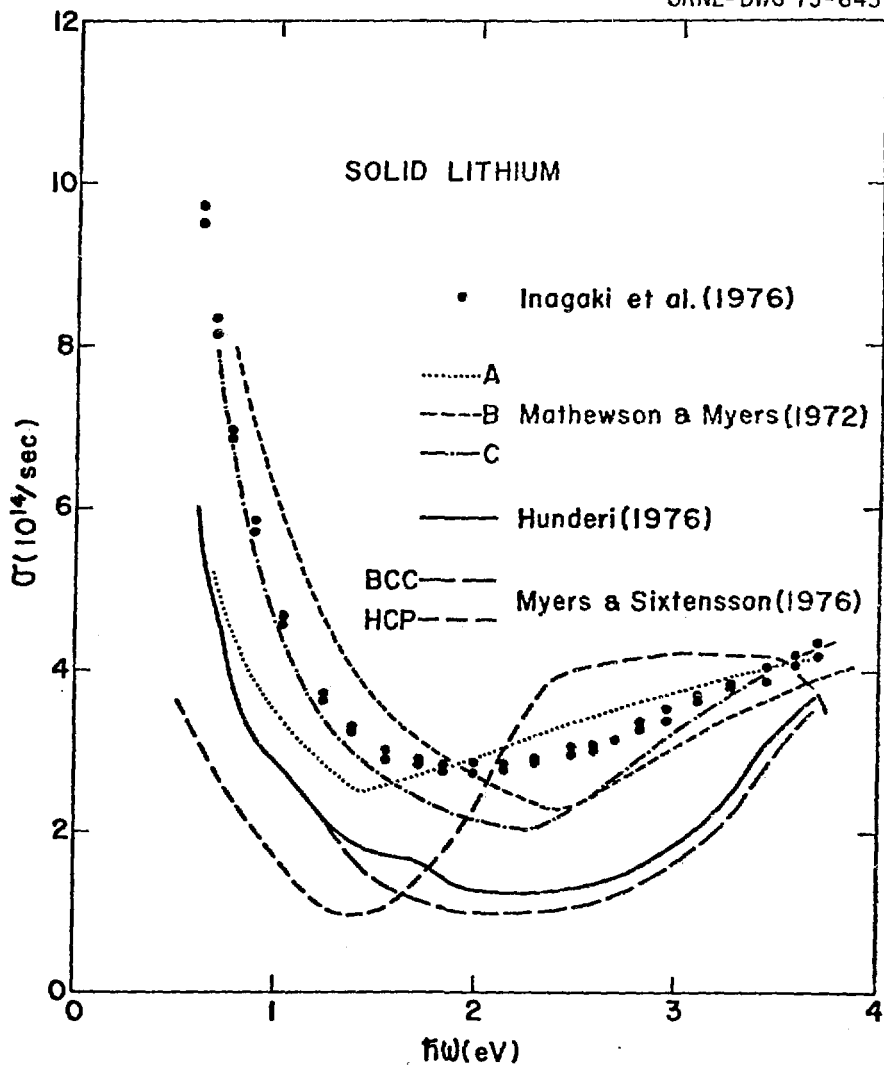


Figure 5

ORNL-DWG 79-15543

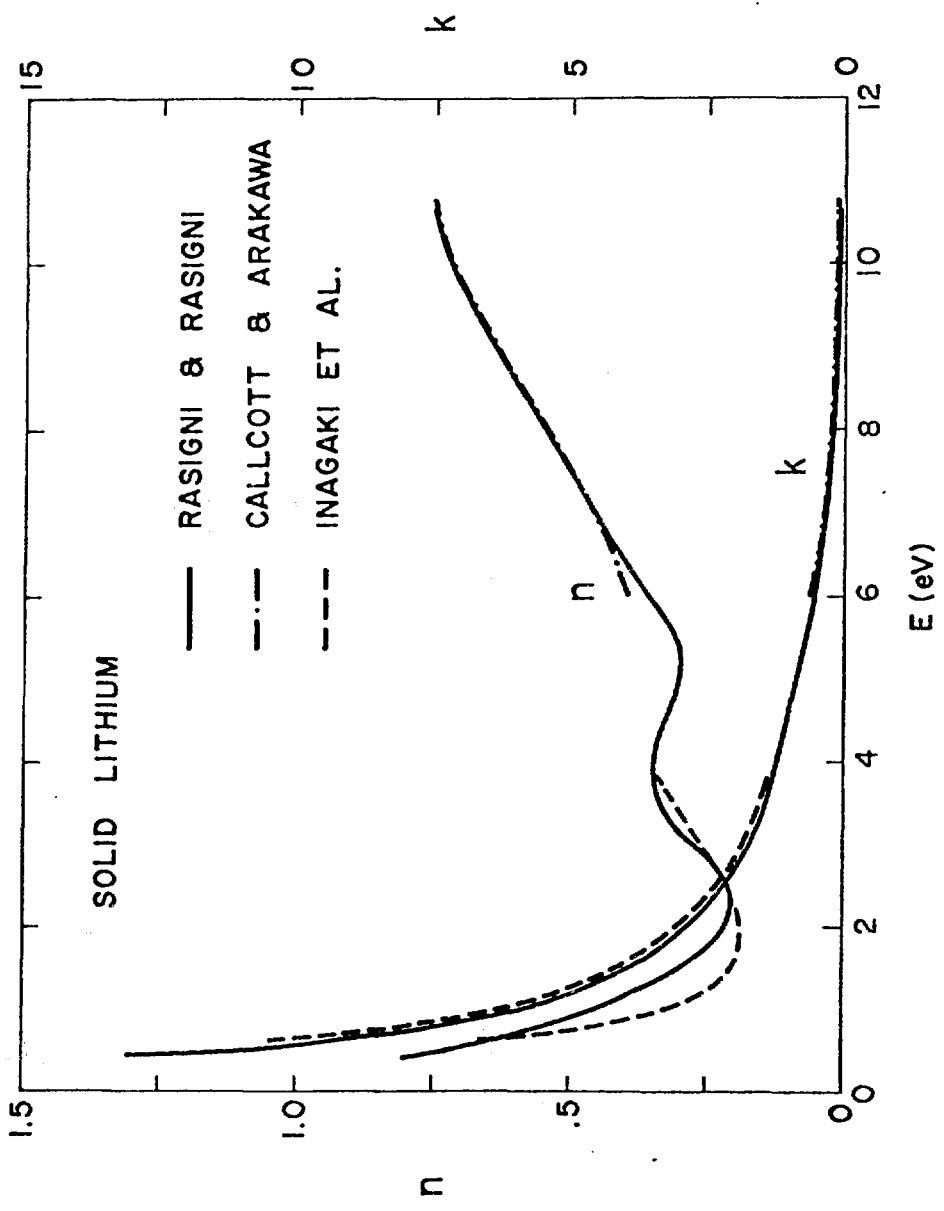


Figure 6

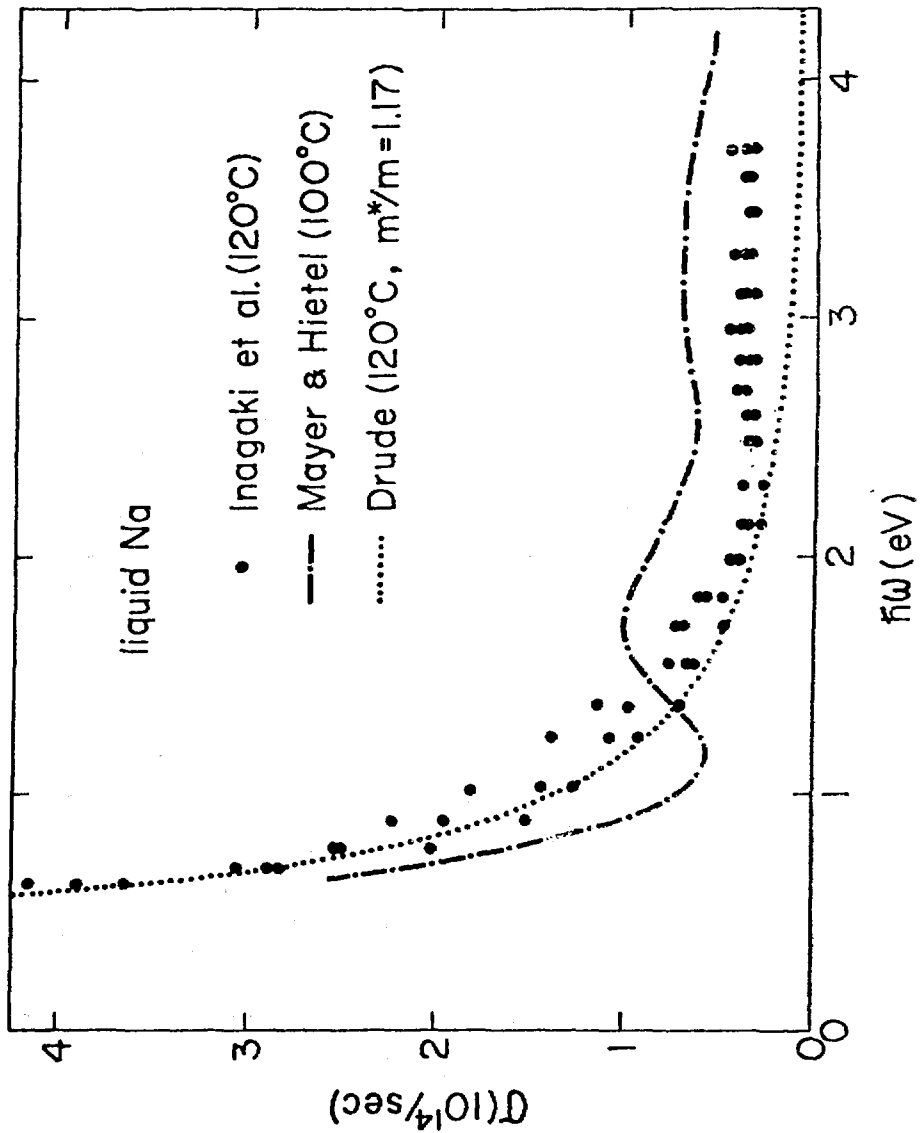


Figure 7

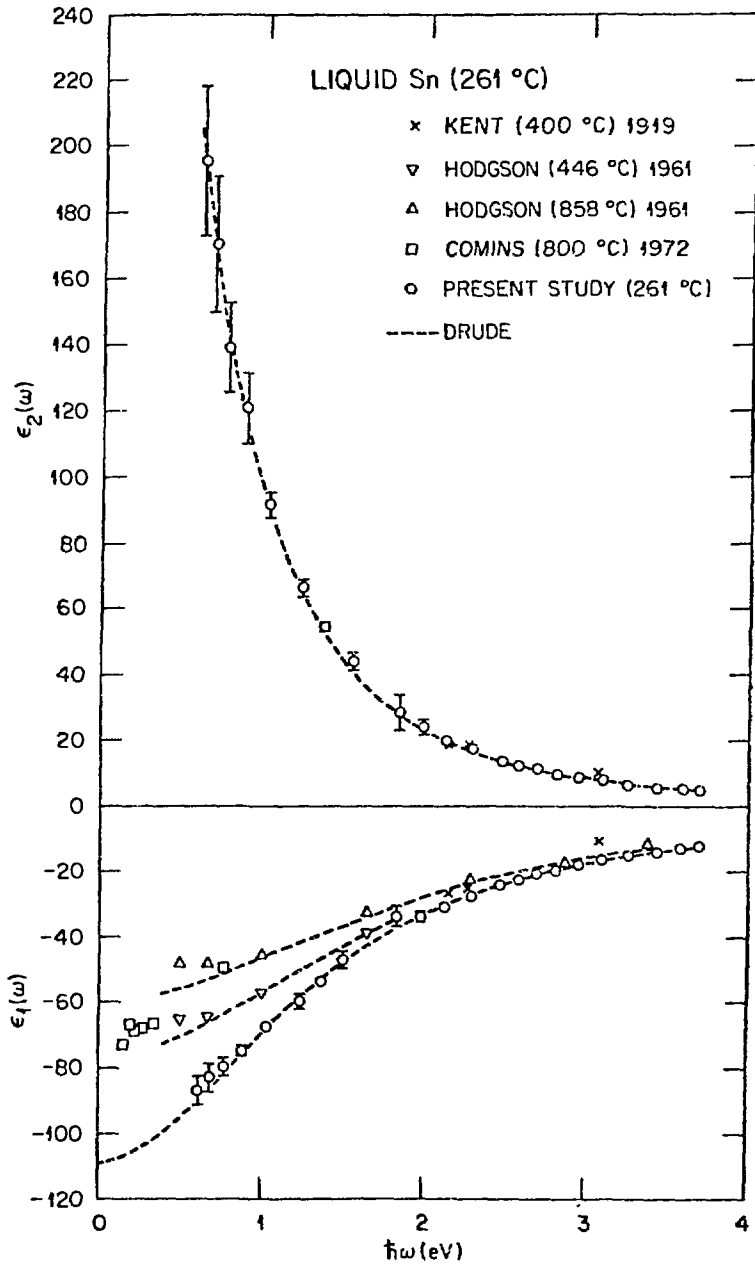


Figure 8

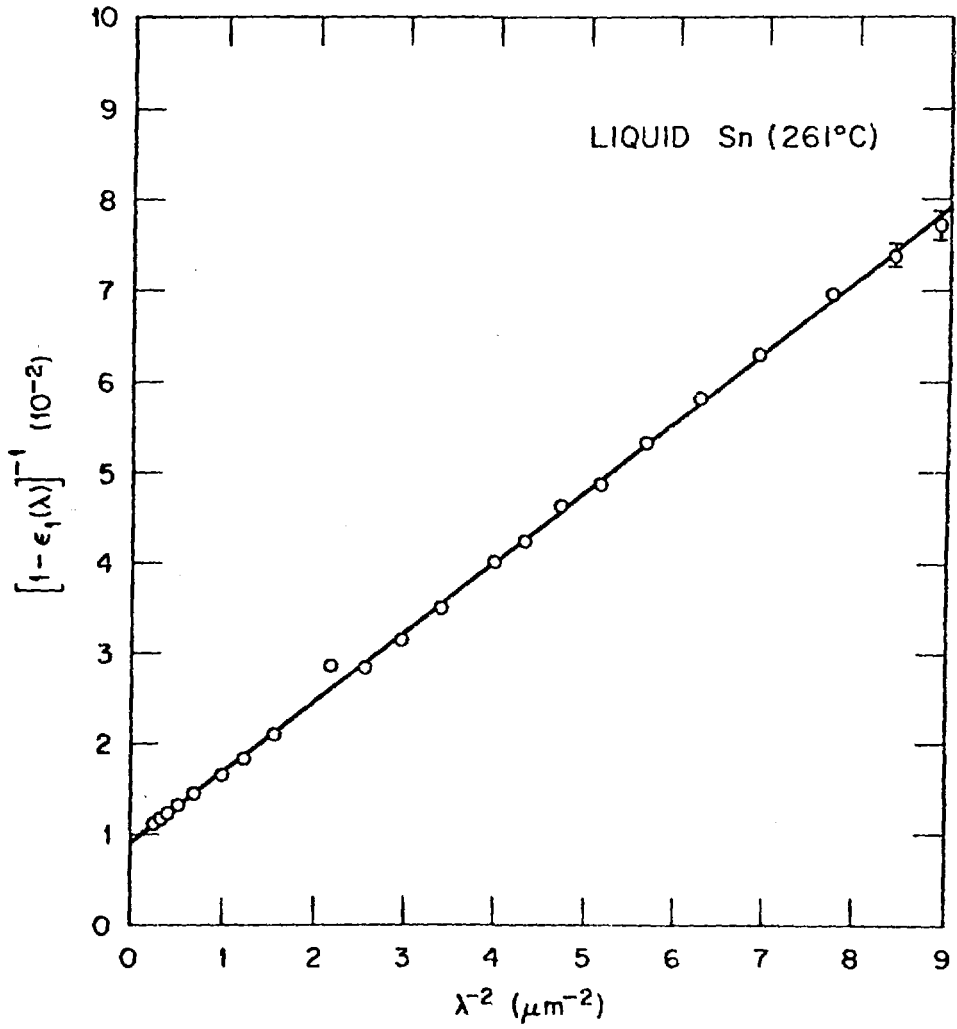


Figure 9

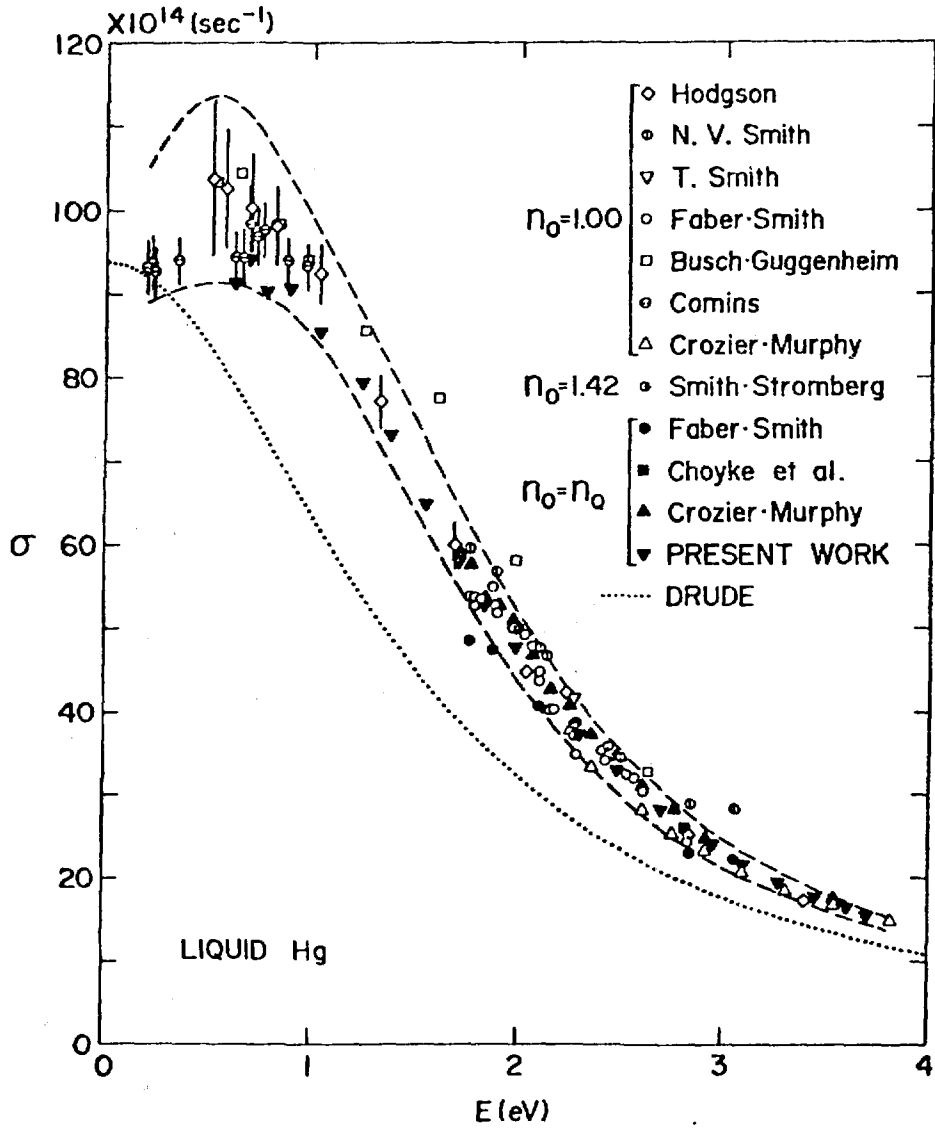


Figure 10

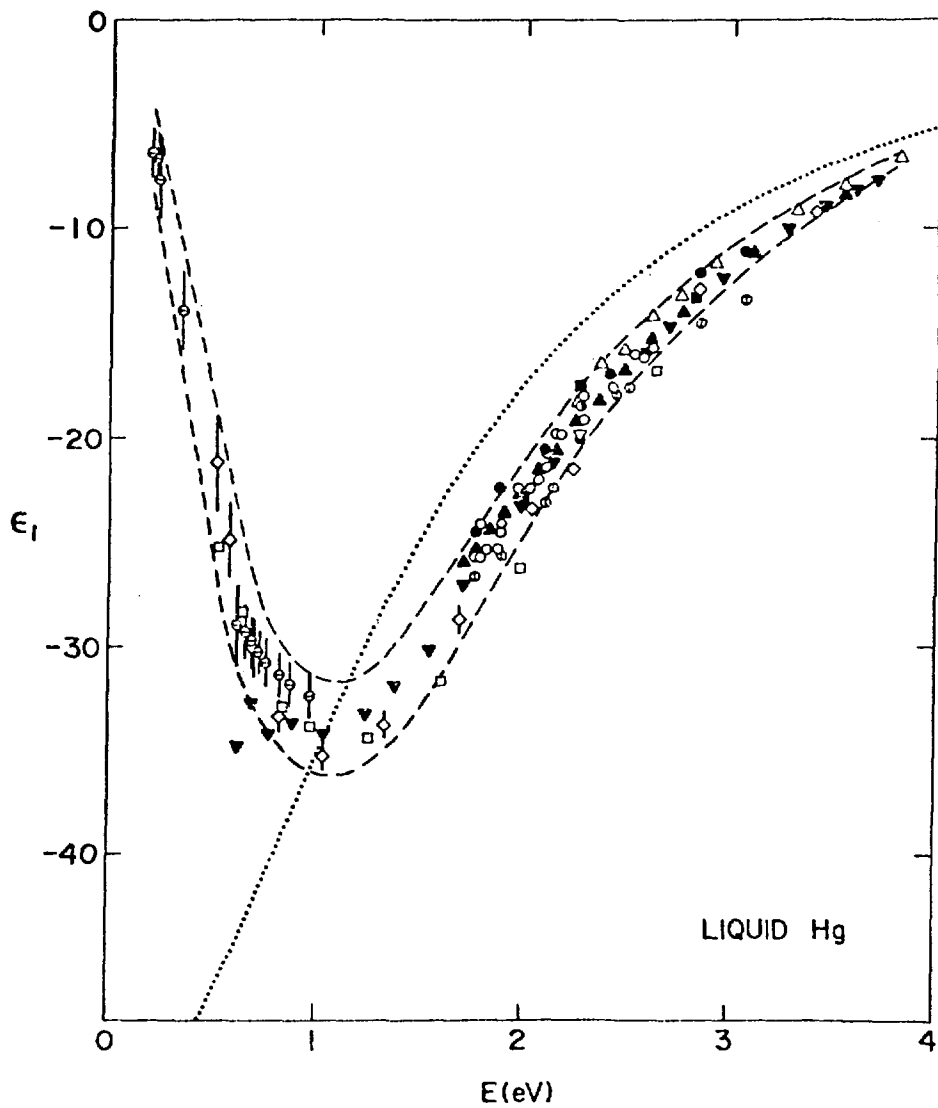


Figure 11

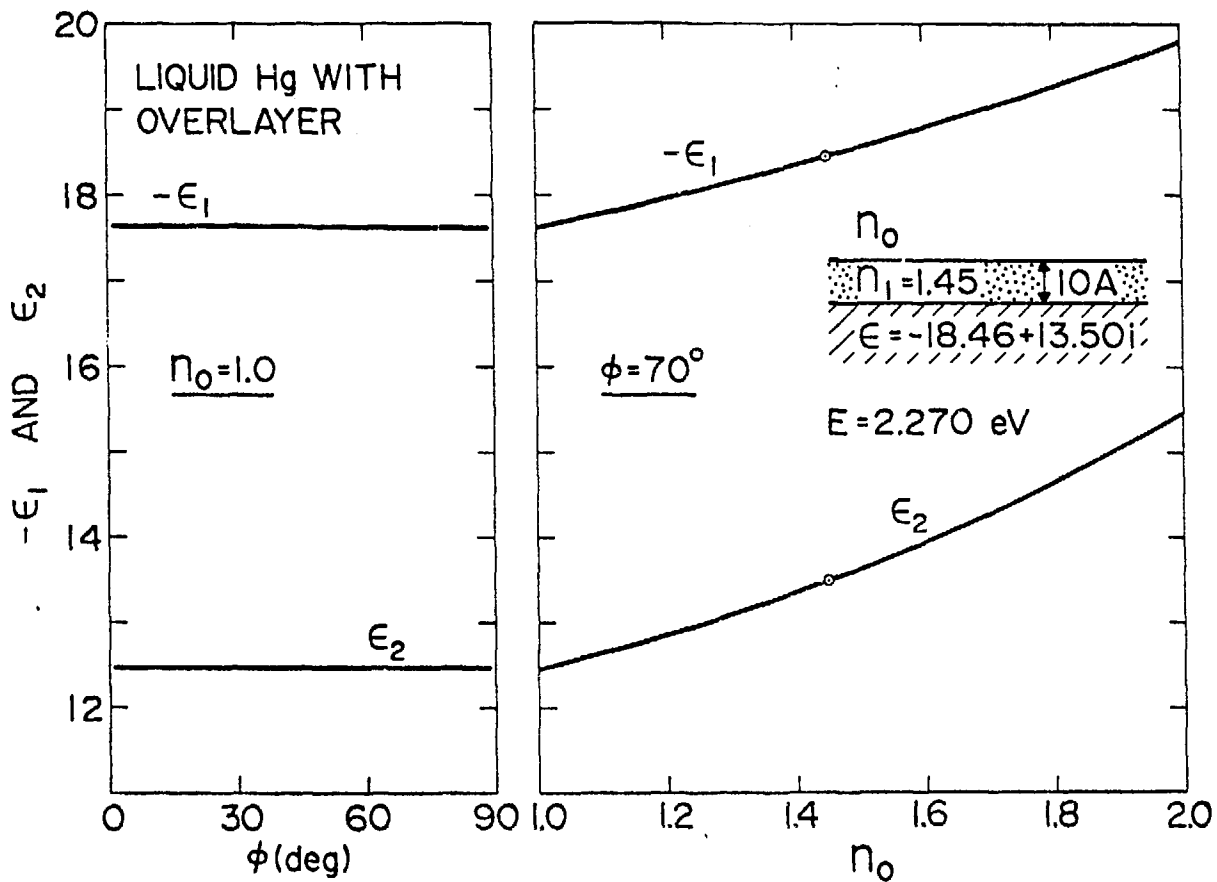


Figure 12

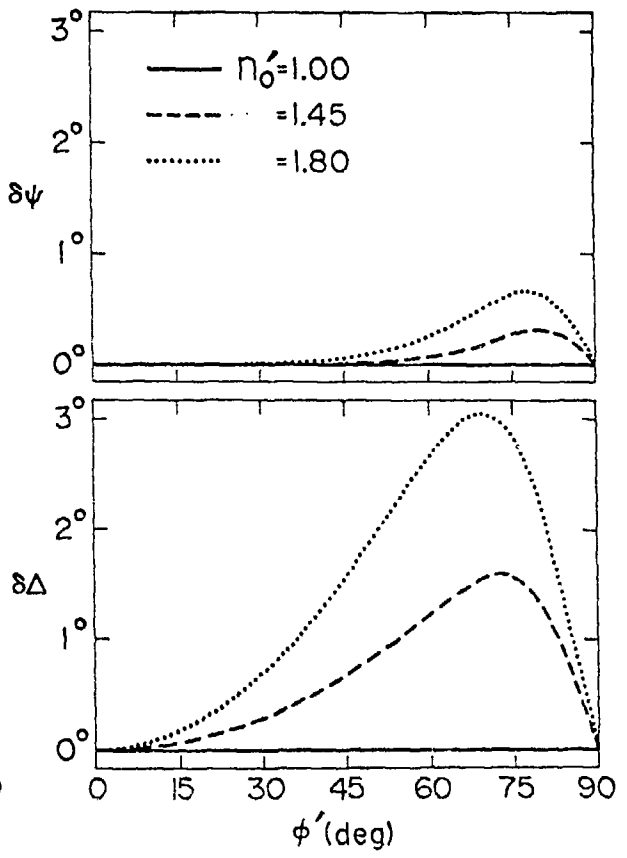
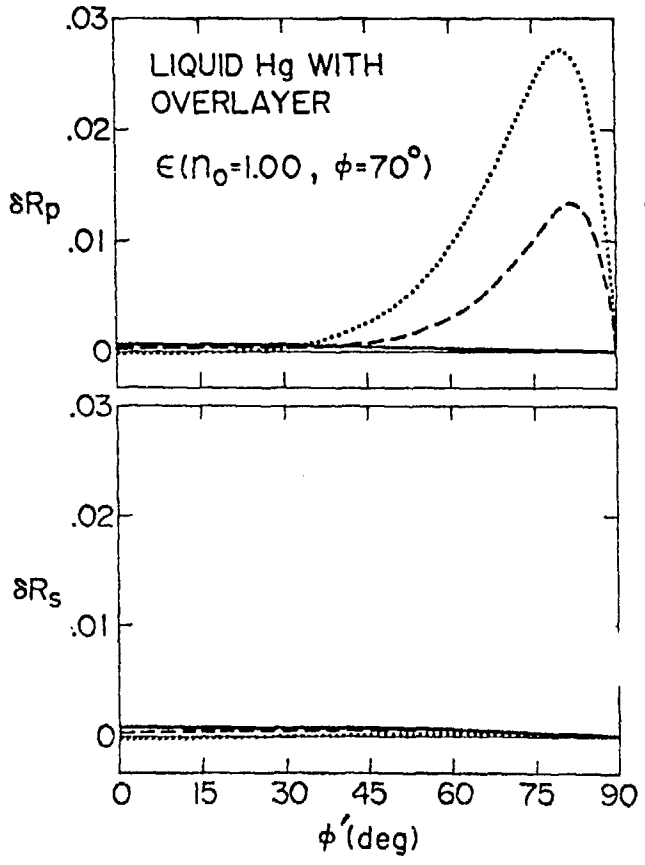


Figure 13

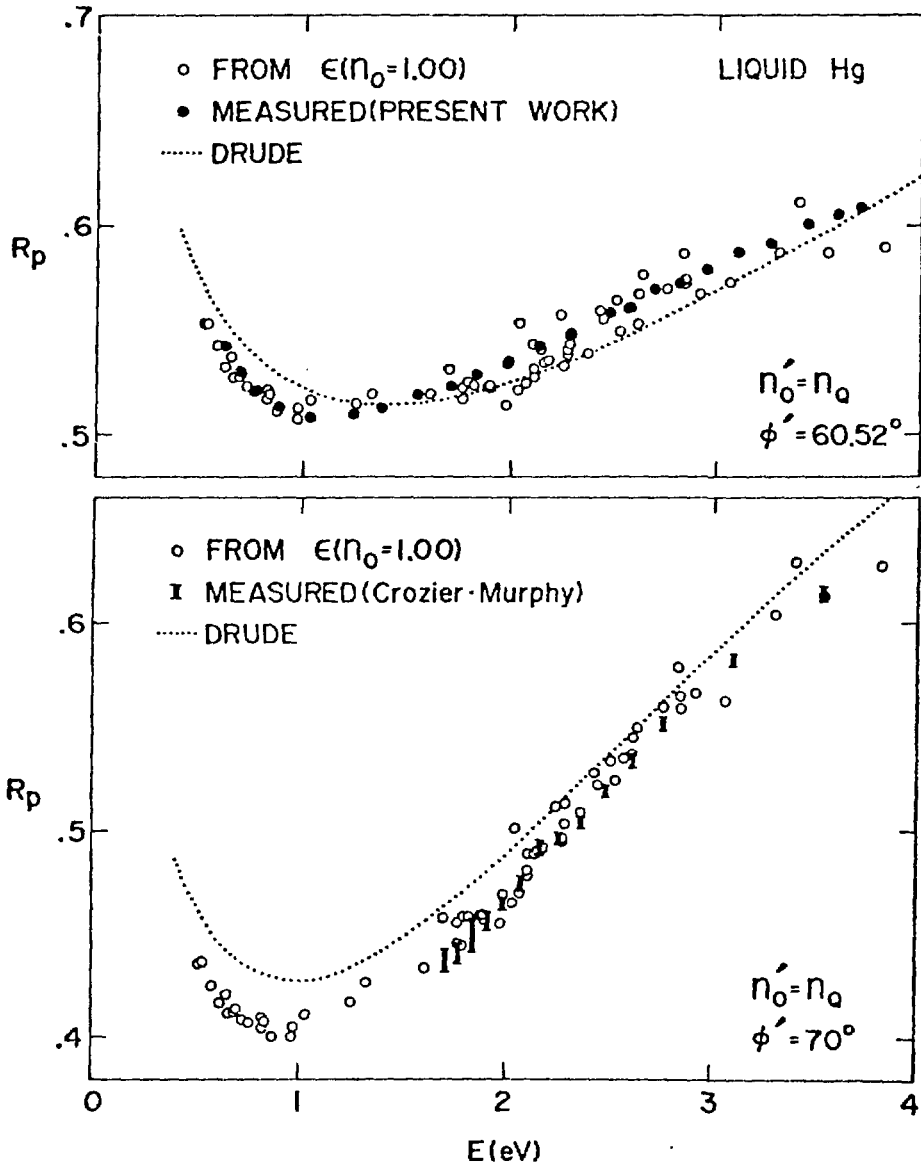


Figure 14

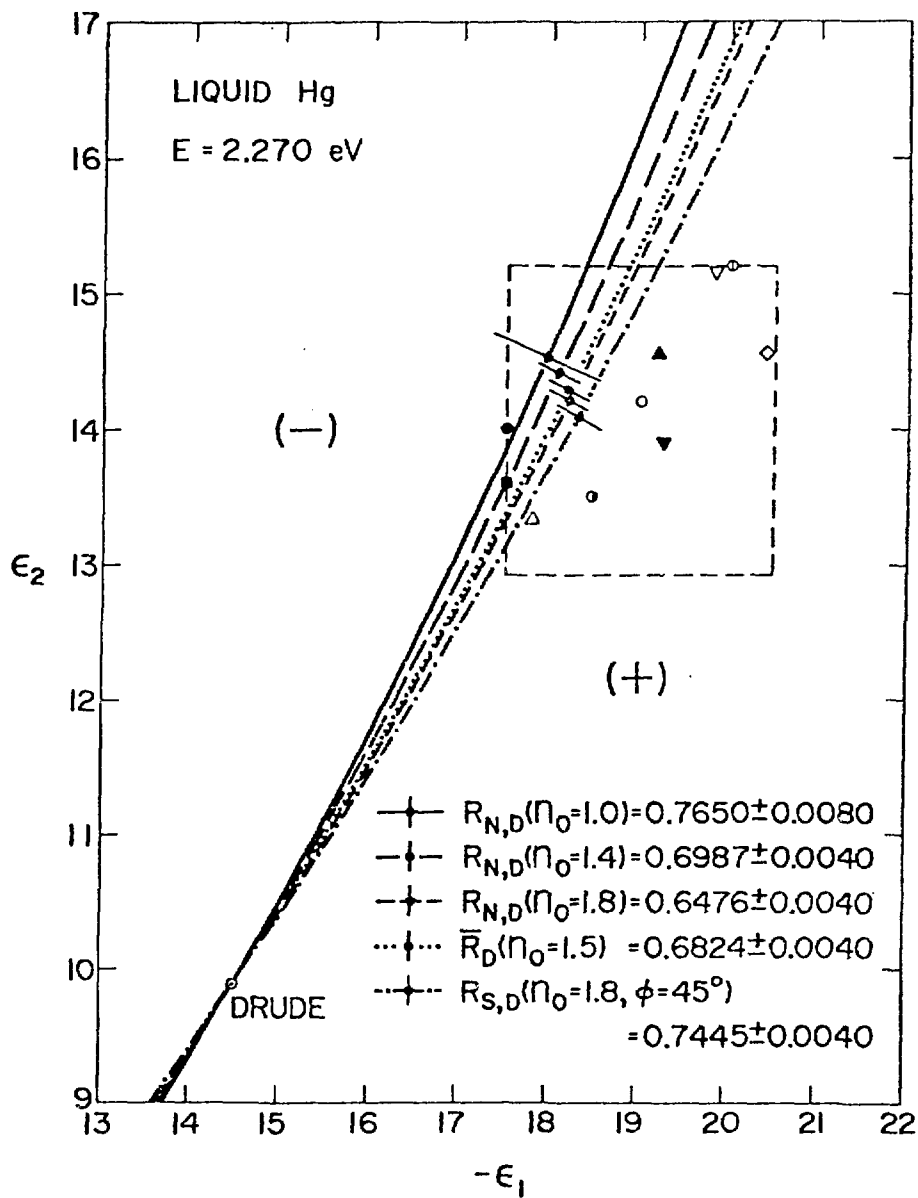


Figure 15

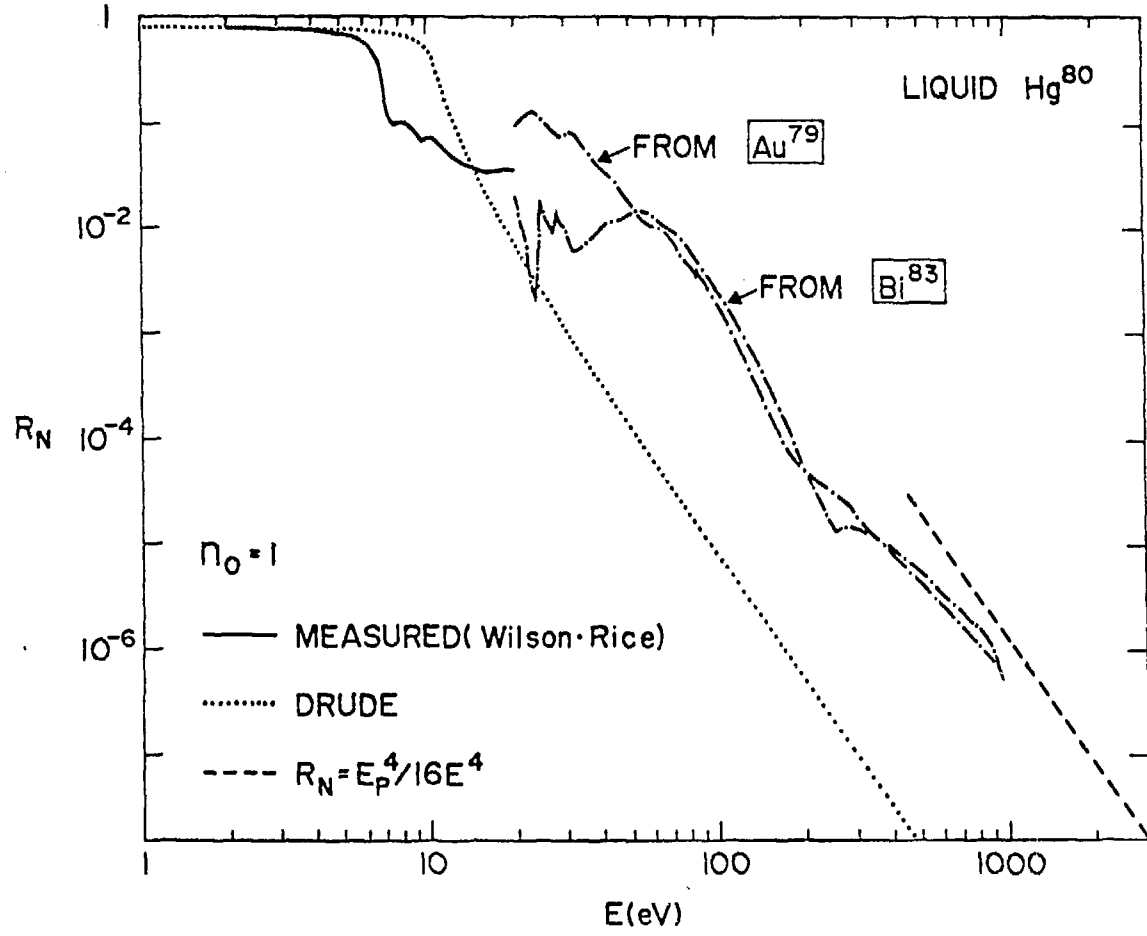


Figure 16

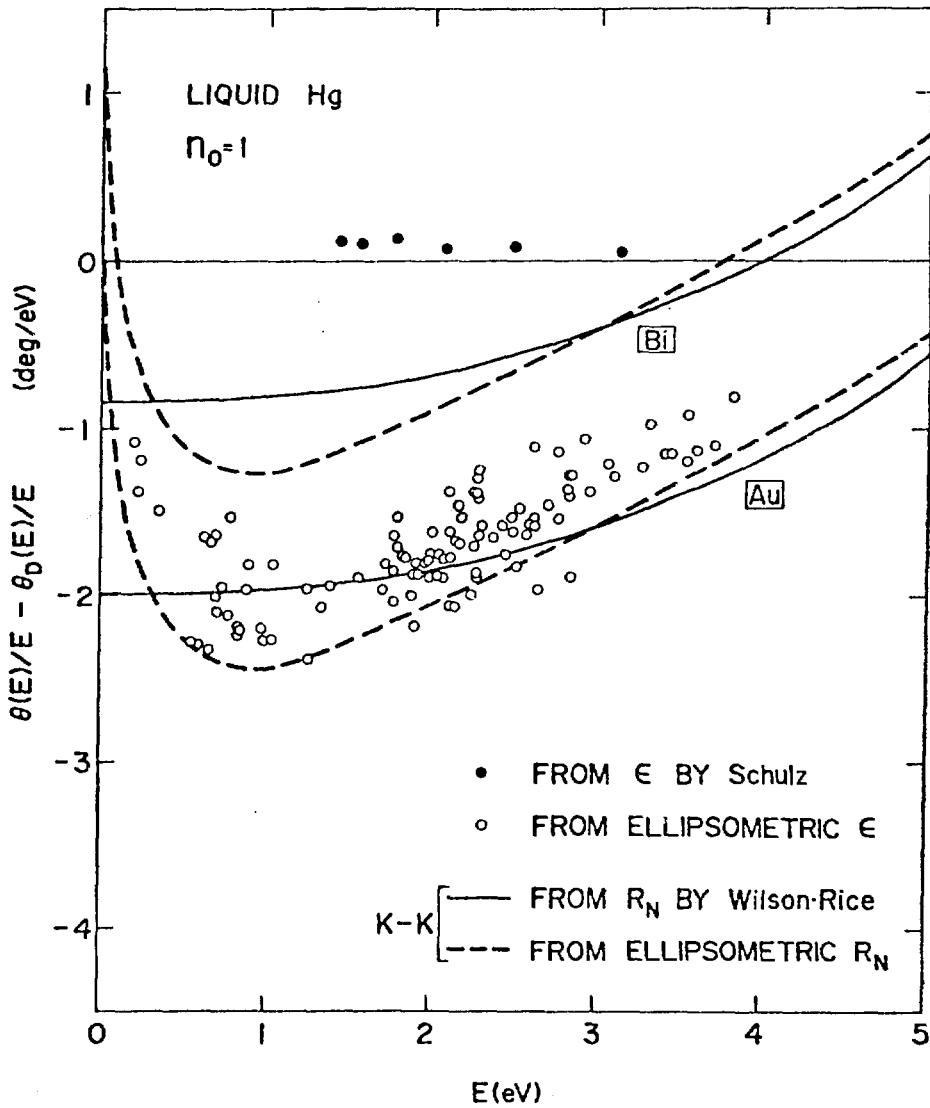


Figure 17